RESEARCH ARTICLE

ADVANCED
MATERIALS
INTERFACES
Open Access

www.advmatinterfaces.de

Bandgap Engineering of TiO$_2$ for Enhanced Selectivity in Photoelectrochemical Glycerol Oxidation

Claudio M. Pecoraro, Siming Wu, Monica Santamaria, and Patrik Schmuki*

The application of photoelectrochemical cells to the partial oxidation of biomass represents a promising avenue as a sustainable process for obtaining valuable products. However, achieving both efficient conversion rates and high selectivity of desired products remains a great challenge. In this study, the photoelectrochemical oxidation of glycerol is investigated to produce dihydroxyacetone (DHA) as the primary target using TiO$_2$ nanotubes (NTs) as the photoanode. Nitrogen doping is used to modify the TiO$_2$ NTs, resulting in enhanced visible light photoactivity in N-doped NTs. These N-doped NTs exhibit a high selectivity toward DHA and show a remarkable faradaic efficiency when irradiated with light at a wavelength of 450 nm, i.e., light that excites N-related states in the band gap of TiO$_2$. The N-doped material also exhibits remarkable stability over prolonged reaction periods. The superior performance of N-doped NTs can be attributed to the band-engineering effects induced by nitrogen doping. Specifically, N-doping leads to an upward shift of the valence band, thereby adjusting the exit energy levels of photogenerated holes that result in a high selectivity toward glycerol conversion to DHA.

1. Introduction

The catalytic oxidation of glycerol, an abundant by-product of biodiesel production, has attracted considerable interest due to the versatile applications of its oxygenated derivatives, such as aldehydes and ketones.[1–4] In particular,

C. M. Pecoraro, S. Wu, P. Schmuki
Department of Materials Science and Engineering
Chair for Surface Science and Corrosion (WW4-LKO)
Friedrich-Alexander-Universität Erlangen-Nürnberg
Martensstraße 7, 91058 Erlangen, Germany
E-mail: schmuki@ww.uni-erlangen.de

C. M. Pecoraro, M. Santamaria
Dipartimento di Ingegneria
Università degli Studi di Palermo
Viale delle Scienze Edificio 6
Palermo 90128, Italy

P. Schmuki
Regional Centre of Advanced Technologies and Materials
Šlechtitelů 27, Olomouc 78371, Czech Republic

The ORCID identification number(s) for the author(s) of this article can be found under https://doi.org/10.1002/admi.202400583

dihydroxyacetone (DHA) and glyceraldehyde (GA) are widely used in industries such as cosmetics, pharmaceuticals, fine chemicals, and food production,[5–7] making the catalytic synthesis of these compounds from glycerol an economically attractive proposition.[8–10] Conventional industrial methods for producing DHA and GA from glycerol through thermo-catalysis require severe conditions, such as high pressure and temperature, and expensive noble-metal catalysts (e.g., Pt, Au, Pd) along with exogenous oxidants like O$_2$ or H$_2$O$_2$.[11–13]

Photoelectrochemical oxidation provides a promising approach, which combines both renewable feedstock and green energy sources together to make building-block chemical and clean fuel at the same time. In PEC systems, photoinduced electrons (e$^-$) and holes (h$^+$) are generated and migrate in the applied electric field, with electrons moving to the cathode and holes migrating to the surfaces of the photoanode. This results in reduction and oxidation reactions occurring at these respective electrodes.[14–16] Despite the numerous investigations of PEC systems in water splitting,[17–20] and the degradation of organic pollutants,[21–23] the investigation of PEC oxidation of organic compounds is relatively poor. The great challenge in PEC oxidation of organic compounds is to achieve high selectivity toward desired products and high faradaic efficiency (FE).

TiO$_2$ has been established as the most widely used photoanode due to its high photocatalytic activity, excellent stability, scalability, low cost, and non-toxic nature.[24–28] However, its photovalue in view in PEC glycerol is limited as the generated holes exiting the electrode leave a high surface energy level that is sufficient to form hydroxyl radicals (·OH) — this strong oxidation power typically leads to complete mineralization of glycerol to CO$_2$ or H$_2$O, thus strongly reducing the FE toward high value-added products such as DHA and GA.

Therefore, in this study, we focus on improving the selectivity and FE of PEC oxidation of glycerol by tuning the band structure of TiO$_2$ toward a milder oxidation condition. To achieve this goal, we subject TiO$_2$ nanotubes to nitrogen doping treatment, resulting in N-doped NTs. We then investigate the conversion of glycerol to the target product DHA and the secondary product GA using both undoped and doped TiO$_2$ photoanodes under UV (365 nm) and visible light (450 nm) irradiation. Our results show that nitrogen doping, as expected,[29,30] induces an upward shift

**ADVANCED
SCIENCE NEWS**

www.advancedsciencenews.com

**ADVANCED
MATERIALS
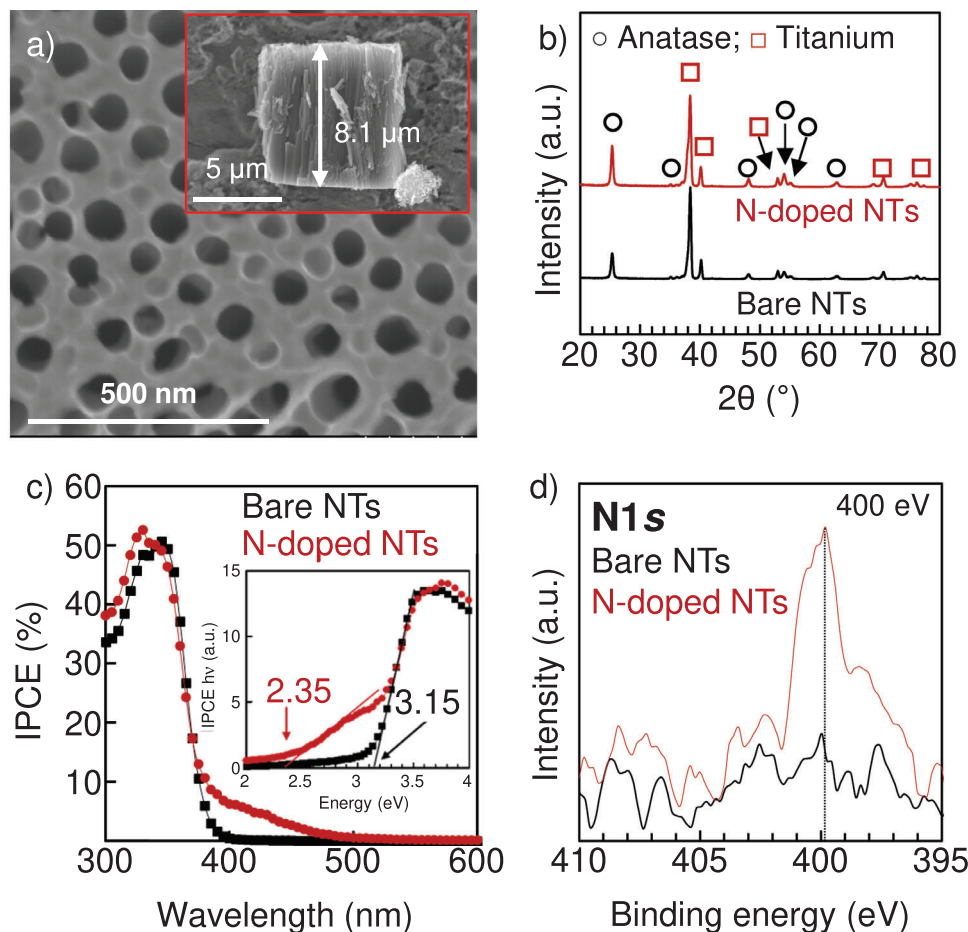INTERFACES**
Open Access

www.advmatinterfaces.de

Figure 1. a) SEM pictures of N-doped NTs. b) XRD patterns, c) IPCE spectra with the respective evaluation of the band gap in the inset, and d) XPS spectra in the N 1s region of TiO_2 NTs before and after N-doping.

in the valence band and narrows the band gap. This allows the use of lower energy light sources and most importantly it reduces the oxidation power of photogenerated h^+, and as a result, it leads to a significantly improved selectivity toward DHA production and a higher FE for glycerol oxidation.

2. Results and Discussion

TiO_2 NTs were first synthesized via anodization of Ti foil using g a voltage of 60 V for 15 min in an ethylene glycol mixture (0.15 M NH_4F, 3 vol% deionized water) with a two-electrode configuration, using the Ti foil as the anode and Pt foil as the cathode. After the anodization step, the as-formed nanotube layers were subjected to annealing in air at 450 °C for 1 h (bare NTs). For nitrogen doping, the samples were exposed to an NH_3 flow in a quartz tube at a furnace temperature of 450 °C for 1 h (N-doped NTs). Further details for the NTs synthesis can be found in the Supporting Information.

Figure S1 (Suppporting Information) shows the SEM images of the bare NTs and **Figure 1a** shows the SEM image of the N-doped NTs. Both bare NTs and N-doped NTs show a self-organized structure with tubes averaging 8 µm in length and ≈60 nm in diameter., i.e., No noticeable variation in morphol-

ogy is observed after N-doping. Additionally, the XRD patterns of both bare NTs and N-doped NTs (Figure 1b) show the characteristic diffraction peaks at $2\theta = 25.3°$ and 48.1°, indicating the presence of the anatase phase.[31,32] These results show that N-doping has a minimal effect on the morphology and crystal structure of TiO_2 NTs.

To characterize the effect of N-doping, we investigated the photoelectrochemical behavior and light reflectance properties. Figure 1c shows the incident photon-to-current conversion efficiency (IPCE) spectra for the TiO_2 NTs before and after N-doping measured in 0.1 M Na_2SO_4 at 0.5 V (vs Ag/AgCl). In both cases, a maximum IPCE value of 50% is observed under UV illumination at a wavelength of ≈330 nm. In the visible light region, N-doped NTs lead to a tail photoresponse up to 400–450 nm, well in line with the literature.[29,33] If the data is plotted according to an indirect optical transition (inset of Figure 1c), a band gap (E_g) of 3.15 eV can be determined for the bare NTs, which is typical for anatase TiO_2.[34] After N-doping, the E_g was determined to be 2.35 eV, which is generally attributed to the shift of the valence band (VB) to a lower energy level by N-doping.[35] Mott-Schottky (M-S) measurements were then conducted to determine the flat band potential (V_{FB}), and the results are depicted in Figure S2 (Suppporting Information) for
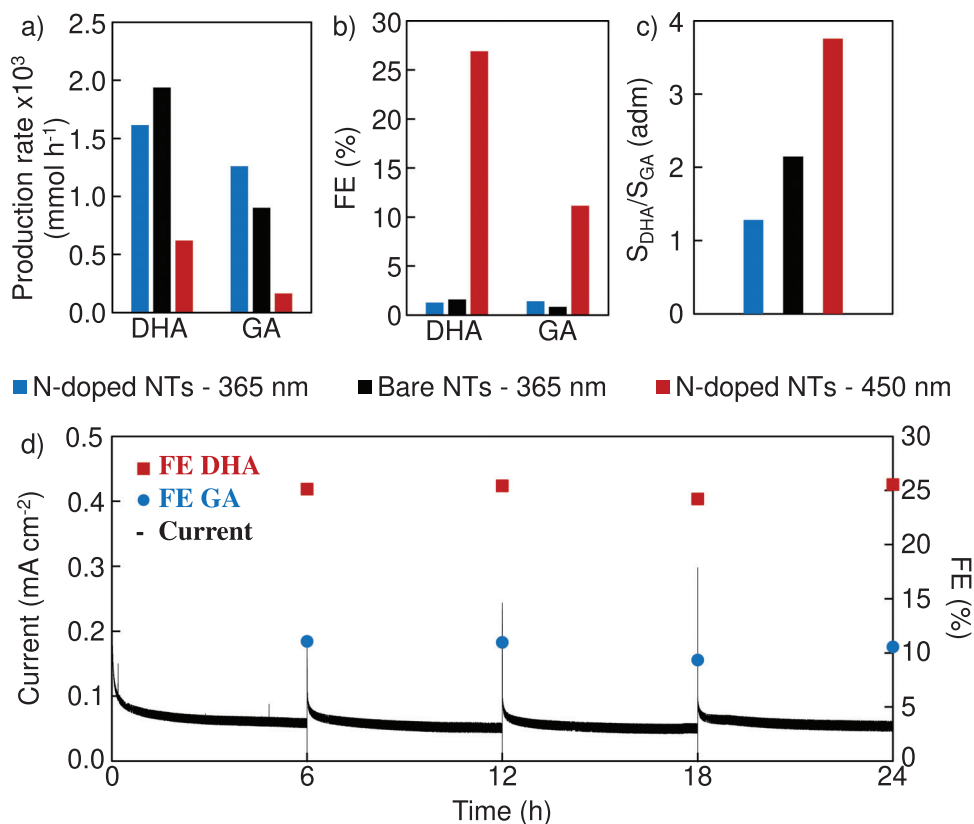
2400583 (2 of 6)

Figure 2. a) production rate and b) FE of DHA and GA after 4 h of irradiation with 365 or 450 nm LED by using TiO_2 NTs before and after N-doping. The final DHA/GA ratio is reported in c). d) stability test carried out by irradiating the N-doped NTs with 450 nm LED.

both the TiO_2 NTs before and after N-doping. In both cases, a value of -0.7 V versus Ag/AgCl was obtained, aligning with findings in the literature.[28,36,37] UV–vis spectra (Figure S3, Supporting Information) further confirm the visible light adsorption of N-doped NTs. XPS analysis is also performed to investigate the chemical composition of the bare and N-doped NTs, the spectra are shown in Figure 1d and Figure S4 (Supporting Information). For both bare and N-doped NTs, the Ti $2p$ spectra show the Ti-doublet at 458.7 and 464.5 eV, and the O $1s$ XPS spectra show one peak at 530 eV, which are attributed to the Ti-O bond., i.e., N-doping doesn't affect the chemical state of Ti and O in TiO_2. In the N $1s$ XPS spectra (Figure 1d), a distinct peak at 399.8 eV appears in the N-doped NTs, which in line with literature,[38] can be attributed to the incorporation of N atoms into the TiO_2 lattice, forming an O–Ti–N structural feature. This observation suggests that N atoms are doped by substituting oxygen atoms in the lattice, rather than chemisorbed nitrogen species on the surface of the TiO_2 NTs. In addition, an N doping amount of 0.7 at% is determined by XPS.

The photoelectrochemical behavior of TiO_2 photoanodes was investigated in a glycerol electrolyte under irradiation at wavelengths of either 365 or 450 nm, focusing on the selectivity toward the glycerol oxidation products DHA and GA. **Figure 2a** and Figures S5–S7 (Supporting Information) illustrate the DHA and GA production rates over bare NTs and N-doped NTs at a constant potential of 0.5 V versus Ag/AgCl in a 0.1 M Na_2SO_4 electrolyte with 0.1 M glycerol over 4 h. The oxidation products were quantitatively analyzed by high-performance liquid chromatography (HPLC). A higher production rate of DHA over GA is observed under all conditions, indicating a preferential conversion of glycerol to the target product DHA. Under 365 nm irradiation, bare NTs exhibit the highest production rate of DHA due to the intrinsic photoactivity of TiO_2 in the UV region. This is supported by the photocurrent measurements, where bare NTs display higher photocurrent than N-doped NTs under 365 nm LED illumination (Figures S5 and S6, Supporting Information). A remarkable difference is observed under 450 nm LED irradiation for N-doped NTs., i.e., despite a decrease in photocurrent (Figures S7, Supporting Information), the FEs for both DHA and GA increase significantly, with DHA showing a more pronounced rise, reaching up to 27% and 11%, respectively (Figure 2b). This observation, in contrast to the efficiencies under 365 nm irradiation where the FEs remained below 2% (see Table S1, Supporting Information), underscores a more effective charge utilization in glycerol conversion under visible light by N-doped NTs. The selectivity of DHA over GA was further evaluated by calculating the ratio of their production (Figures S8, Supporting Information). Remarkably, N-doped NTs irradiated with 450 nm LED exhibit the highest selectivity for DHA among all the conditions, as evidenced by the calculated ratio of their production detailed in Table S1 (Supporting Information) and illustrated in Figure 2c. Additionally, the results of photon-to-chemical conversion efficiency (Table S2, Supporting Information) show that N-doped NTs under 450 nm irradiation achieve a comparable
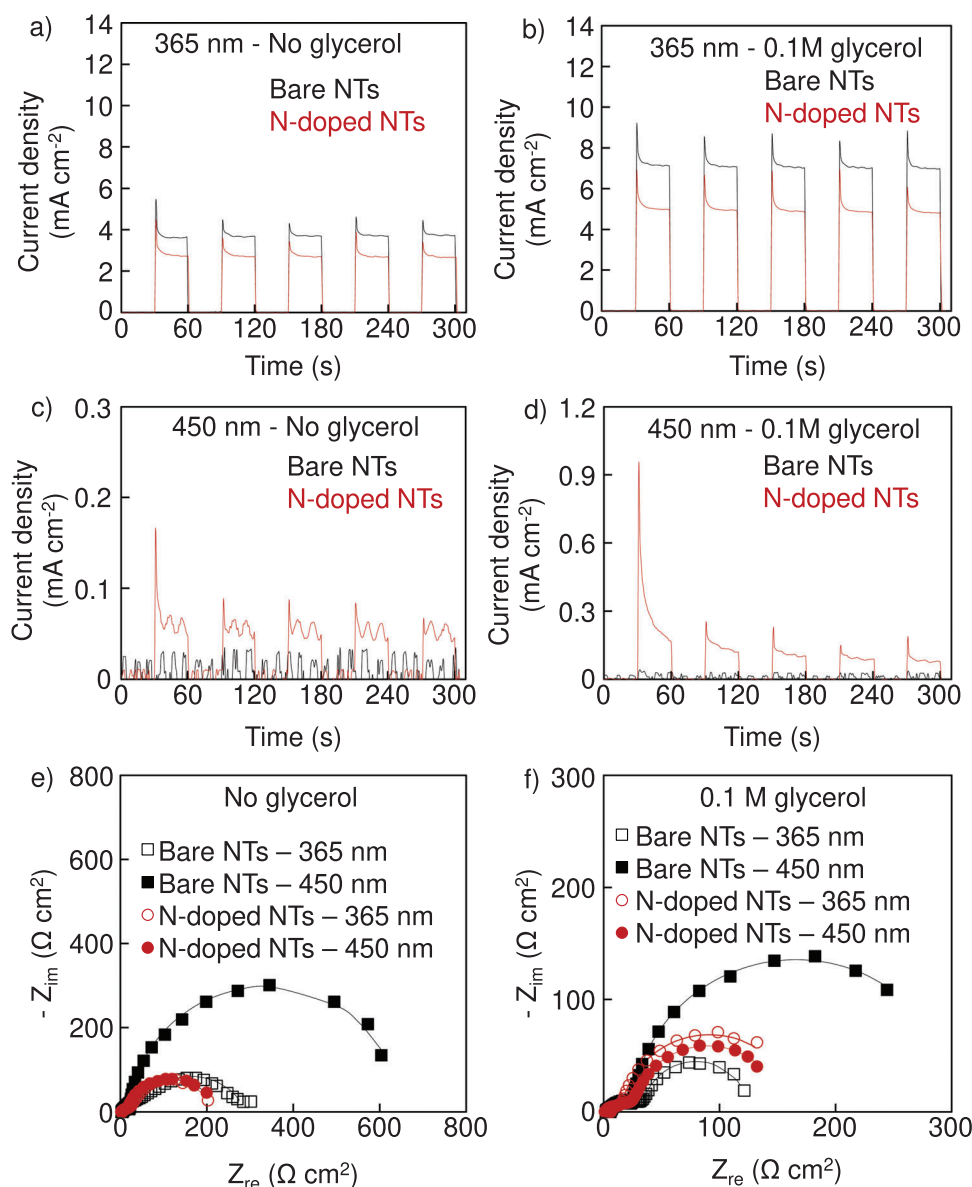
**ADVANCED
SCIENCE NEWS**

www.advancedsciencenews.com

**ADVANCED
MATERIALS
INTERFACES**
Open Access

www.advmatinterfaces.de

Figure 3. Photocurrent transients were recorded without a,c) and with 0.1 M glycerol b,d) by irradiating the TiO$_2$ NTs before and after N-doping with 365 or 450 nm LED. EIS spectra recorded without and with 0.1 M glycerol are reported in e,f), respectively, using TiO$_2$ NTs before or after N-doping and irradiating the sample with 365 or 450 nm LED.

conversion of photons to chemicals compared to UV experiments, despite the visible light utilization and exhibiting a lower measured photocurrent.

The stability of N-doped NTs was also evaluated by 24 h long-term experiments under 450 nm LED illumination, and the results are shown in Figure 2d. N-doped NTs show a consistent photocurrent and FE toward DHA and GA, and no structural changes are observed in N-doped NTs after the test (Figure S9, Suppporting Information), indicating their excellent stability.

To obtain some further insight into the different PEC glycerol oxidation behavior of bare NTs and N-doped NTs, we performed transient photocurrent measurement and electrochemical impedance spectroscopy (EIS) under 365 and 450 nm LED light irradiation in both aqueous and glycerol-containing solu-

tion. The transient photocurrent results (**Figure 3a,b**) show that under 365 nm LED irradiation, both bare and N-doped NTs experience an increase in photocurrent with the addition of 0.1 M glycerol, confirming the role of glycerol as an effective hole-trapping agent. However, bare NTs consistently exhibit higher photocurrents than N-doped NTs under these conditions. In contrast, under 450 nm LED light, the photocurrent behavior diverges significantly (Figure 3c,d). N-doped NTs exhibit a noticeable photocurrent that is further enhanced by the addition of glycerol, confirming its visible light activity. Conversely, bare NTs exhibit a negligible photocurrent that is unaffected by the addition of glycerol. This contrast highlights the superior visible light response of N-doped NTs. EIS measurements (Figure 3e,f; Figure S10, Suppporting Information) show that light exposure significantly
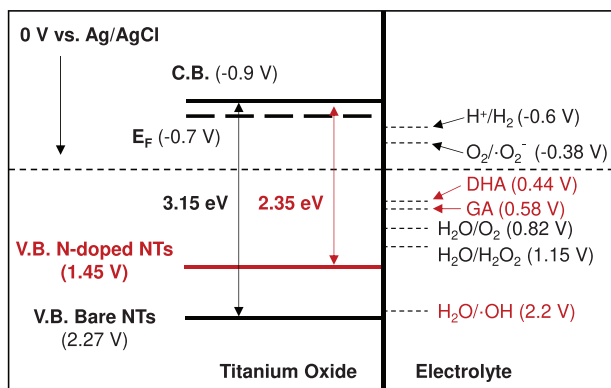
**ADVANCED
SCIENCE NEWS**

www.advancedsciencenews.com

**ADVANCED
MATERIALS
INTERFACES**

www.advmatinterfaces.de

Figure 4. Sketch of the energetic levels of the oxide/electrolyte interface.

reduces the charge transfer resistance (R_{ct}) for all samples, highlighting the critical role of irradiation in facilitating charge generation and transfer. In the presence of glycerol, there is a further reduction in R_{ct} for both types of NTs. In particular, under 365 nm LED, bare NTs show the lowest R_{ct}, while under 450 nm they show the highest R_{ct}. Meanwhile, N-doped NTs maintain low R_{ct} values under both wavelengths, confirming their effective charge transfer properties, especially under visible light. These results illustrate that the improved PEC glycerol oxidation performance in N-doped NTs is due to the high visible light utilization and enhanced charge transfer efficiency for the N-doped material.

Based on the above data (details in the Supporting Information), an energetic sketch was constructed and is shown in **Figure 4** to illustrate the impact of N-doping on the band structure and the resulting photoelectrocatalytic effects. The preferential formation of DHA over GA during glycerol oxidation can be attributed to the lower oxidation potential of DHA (0.44 V vs Ag/AgCl) compared to GA (0.58 V vs Ag/AgCl), determined considering the Gibbs free energy found in the literature[39] (more details are reported in the Suppporting Information). This results in a lower energy input required for the partial oxidation of glycerol to DHA, thus favoring its selective formation.

As indicated by the band alignment, both water splitting and glycerol oxidation are energetically favorable processes for bare and N-doped NTs. However, the energy level of the VB in bare NTs is higher than the energy required to generate ·OH, facilitating the production of these highly reactive radicals. This leads to the preferential oxidation of glycerol to smaller, more oxidized products, ultimately resulting in the complete mineralization of glycerol to CO_2 and H_2 and consequently low FE for DHA and GA. In contrast, the VB of N-doped NTs is below the energy required to generate ·OH, which suppresses the formation of these radicals and thus shifts the glycerol oxidation pathway toward the production of partial oxidation products such as DHA and GA. The suppression of ·OH radicals under 450 nm light irradiation in N-doped NTs was further examined through a ·OH scavenger degradation test using tert-butanol,[40] as shown in Figure S11 (Suppporting Information). Under 365 nm light irradiation, tert-butanol degradation was similar in the case of both bare and N-doped NTs. Notably, N-doped NTs irradiated with 450 nm light show negligible tert-butanol degradation, suggesting minimal hydroxyl radical formation. This implies that the valence band

holes are not sufficiently oxidizing to produce hydroxyl radicals, enabling selective partial oxidation of glycerol to DHA and GA, thereby improving faradaic efficiency for these high-value products. Therefore, modifying the electronic band structure of TiO_2 by nitrogen doping effectively tunes the reaction pathway of glycerol oxidation and increases the selectivity of the oxidation products.

3. Conclusion

In this study, we investigated the efficiency of N-doped NTs for the photoelectrochemical oxidation of glycerol to produce DHA and GA. The N-doped NTs exhibit superior FE under 450 nm irradiation, with 27% for DHA and 11% for GA. They also show remarkable long-term stability. The key factor behind this performance is the significant shift in the valence band energy caused by N-doping, which effectively narrows the band gap. This adjustment allows for the harvesting of visible light and suppresses the formation of hydroxyl radicals, thereby reducing undesired complete glycerol mineralization. In summary, the results highlight the effectiveness of the bandgap engineering approach to modify the selectivity of electrochemical reactions on semiconductors. This method can effectively fine-tune the performance of PEC oxidation reactions of organic compounds, thereby improving selectivity and, as shown for glycerol oxidation, facilitating the production of high-value-added products.

Supporting Information

Supporting Information is available from the Wiley Online Library or from the author.

Conflict of Interest

The authors declare no conflict of interest.

Data Availability Statement

The data that support the findings of this study are available from the corresponding author upon reasonable request.

[1] T. A. Werpy, J. E. Holladay, J. F. White, *Top Value Added Chemicals From Biomass: I. Results of Screening for Potential Candidates from Sugars and Synthesis Gas*, Pacific Northwest National Lab, Richland, WA, **2004**.

[2] P. Gallezot, *Chem. Soc. Rev.* **2012**, *41*, 1538.

[3] J. C. Serrano-Ruiz, R. Luque, A. Sepúlveda-Escribano, *Chem. Soc. Rev.* **2011**, *40*, 5266.

[4] Q. Shi, H. Duan, *Chem Catalysis* **2022**, *2*, 3471.

[5] J. Yu, J. González-Cobos, F. Dappozze, F. J. López-Tenllado, J. Hidalgo-Carrillo, A. Marinas, P. Vernoux, A. Caravaca, C. Guillard, *Appl. Catal. B* **2022**, *318*, 121843.

[6] C. M. Pecoraro, M. Bellardita, V. Loddo, F. Di Franco, L. Palmisano, M. Santamaria, *J. Industr. and Engin. Chem.* **2023**, *118*, 247.

[7] C. Espro, E. Paone, F. Mauriello, R. Gotti, E. Uliassi, M. L. Bolognesi, D. Rodríguez-Padrón, R. Luque, *Chem. Soc. Rev.* **2021**, *50*, 11191.

[8] L. Luo, W. Chen, S.-M. Xu, J. Yang, M. Li, H. Zhou, M. Xu, M. Shao, X. Kong, Z. Li, H. Duan, *J. Am. Chem. Soc.* **2022**, *144*, 7720.

[9] L. Fan, B. Liu, X. Liu, N. Senthilkumar, G. Wang, Z. Wen, *Energy Technology* **2021**, *9*, 2000804.

[10] R. Ciriminna, A. Fidalgo, L. M. Ilharco, M. Pagliaro, *ChemistryOpen* **2018**, *7*, 233.

[11] P. S. Kong, M. K. Aroua, W. M. A. W. Daud, *Renewable Sustainable Energy Rev.* **2016**, *63*, 533.

[12] A. M. Verma, L. Laverdure, M. M. Melander, K. Honkala, *ACS Catal.* **2022**, *12*, 662.

[13] Y. Liu, M. Wang, B. Zhang, D. Yan, X. Xiang, *ACS Catal.* **2022**, *12*, 6946.

[14] M. Grätzel, *Nature* **2001**, *414*, 338.

[15] S. Pitchaimuthu, K. Sridharan, S. Nagarajan, S. Ananthraj, P. Robertson, M. F. Kuehnel, Á. Irabien, M. Maroto-Valer, *Energies (Basel)* **2022**, *15*, 7399.

[16] Y. H. Li, F. Zhang, Y. Chen, J. Y. Li, Y. J. Xu, *Green Chem.* **2020**, *22*, 163.

[17] T. Yao, X. An, H. Han, J. Q. Chen, C. Li, *Adv. Energy Mater.* **2018**, *8*, 1800210.

[18] A. Mehtab, S. M. Alshehri, T. Ahmad, *ACS Appl. Nano Mater.* **2022**, *5*, 12656.

[19] H. Zhou, D. Zhang, H. Xie, Y. Liu, C. Meng, P. Zhang, F. Fan, R. Li, C. Li, *Adv. Mater.* **2023**, *35*, 2300914.

[20] S. M. Wu, L. Wu, N. Denisov, Z. Badura, G. Zoppellaro, X. Y. Yang, P. Schmuki, *J. Am. Chem. Soc.* **2024**, *146*, 16363.

[21] H. Wang, Y. Liang, L. Liu, J. Hu, P. Wu, W. Cui, *Appl. Catal. B* **2017**, *208*, 22.

[22] P. Alulema-Pullupaxi, P. J. Espinoza-Montero, C. Sigcha-Pallo, R. Vargas, L. Fernández, J. M. Peralta-Hernández, J. L. Paz, *Chemosphere* **2021**, *281*, 130821.

[23] W. Chen, S. Liu, Y. Fu, H. Yan, L. Qin, C. Lai, C. Zhang, H. Ye, W. Chen, F. Qin, F. Xu, X. Huo, H. Qin, *Coord. Chem. Rev.* **2022**, *454*, 214341.

[24] X. Chen, S. S. Mao, *Chem. Rev.* **2007**, *107*, 2891.

[25] C. M. Pecoraro, M. Bellardita, V. Loddo, D. Virtù, F. Di Franco, M. Santamaria, *Appl Catal A Gen* **2023**, *650*, 118987.

[26] G. Ognibene, D. A. Cristaldi, R. Fiorenza, I. Blanco, G. Cicala, S. Scirè, M. E. Fragalà, *RSC Adv.* **2016**, *6*, 42778.

[27] S. M. Wu, I. Hwang, B. Osuagwu, J. Will, Z. Wu, B. B. Sarma, F. F. Pu, L. Y. Wang, Z. Badura, G. Zoppellaro, E. Spiecker, P. Schmuki, *ACS Catal.* **2023**, *13*, 33.

[28] C. M. Pecoraro, F. Di Franco, M. Bellardita, V. Loddo, M. Santamaria, *Int. J. Hydrogen Energy* **2024**, *49*, 322.

[29] S. Miraghaei, M. Santamaria, F. Di Quarto, *Electrochim. Acta* **2014**, *134*, 150.

[30] J. M. Macak, A. Ghicov, R. Hahn, H. Tsuchiya, P. Schmuki, *J. Mater. Res.* **2006**, *21*, 2824.

[31] M. Santamaria, G. Conigliaro, F. Di Franco, B. Megna, F. Di Quarto, *J. Electrochem. Soc.* **2017**, *164*, C113.

[32] P. Roy, S. Berger, P. Schmuki, *Angew. Chem., Int. Ed.* **2011**, *50*, 2904.

[33] N. T. Nguyen, S. Ozkan, O. Tomanec, R. Zboril, P. Schmuki, *ChemistryOpen* **2018**, *7*, 131.

[34] D. Kowalski, D. Kim, P. Schmuki, *Nano Today* **2013**, *8*, 235.

[35] M. P. Kumar, R. Jagannathan, S. Ravichandran, *Energy and Fuels* **2020**, *34*, 9030.

[36] D. Regonini, A. Groff, G. D. Sorarù, F. J. Clemens, *Electrochim. Acta* **2015**, *186*, 101.

[37] E. Baran, B. Yazıcı, *Int. J. Hydrogen Energy* **2016**, *41*, 2498.

[38] D. Gao, Z. Lu, C. Wang, W. Li, P. Dong, *Autex Research Journal* **2018**, *18*, 67.

[39] R. P. V. Faria, C. S. M. Pereira, V. M. T. M. Silva, J. M. Loureiro, A. E. Rodrigues, *Ind. Eng. Chem. Res.* **2013**, *52*, 1538.

[40] M. Umair, C. M. Pecoraro, F. Di Franco, M. Santamaria, L. Palmisano, V. Loddo, M. Bellardita, *ChemSusChem* **2024**, 202400404.